SUPPLEMENTARY DATA

Hypothalamic AgRP-neurons control peripheral substrate utilization and nutrient partitioning

.

Aurélie Joly-Amado[1], Raphaël G.P. Denis[1], Julien Castel[1], Amélie Lacombe[1], Céline Cansell[1], Claude Rouch[1], Nadim Kassis[1], Julien Dairou[1], Patrice D. Cani[2], Renée Ventura-Clapier[3], Alexandre Prola[3], Melissa Flamment[4], Fabienne Foufelle[4], Christophe Magnan[1], Serge Luquet[1]

[1]Univ Paris Diderot, Sorbonne Paris Cité, BFA, EAC 4413 CNRS, F-75205 Paris, France

[2]UCL, LDRI, Louvain Drug Research Institute, Université catholique de Louvain, Bruxelles, Belgium

[3]INSERM U-769, Univ Paris-Sud Châtenay-Malabry, F-92296, France

[4]INSERM UMR-S 872, Centre de recherche Faculté de Médecine Pierre et Marie Curie, Université Paris 6, Paris, France

Supplemental results

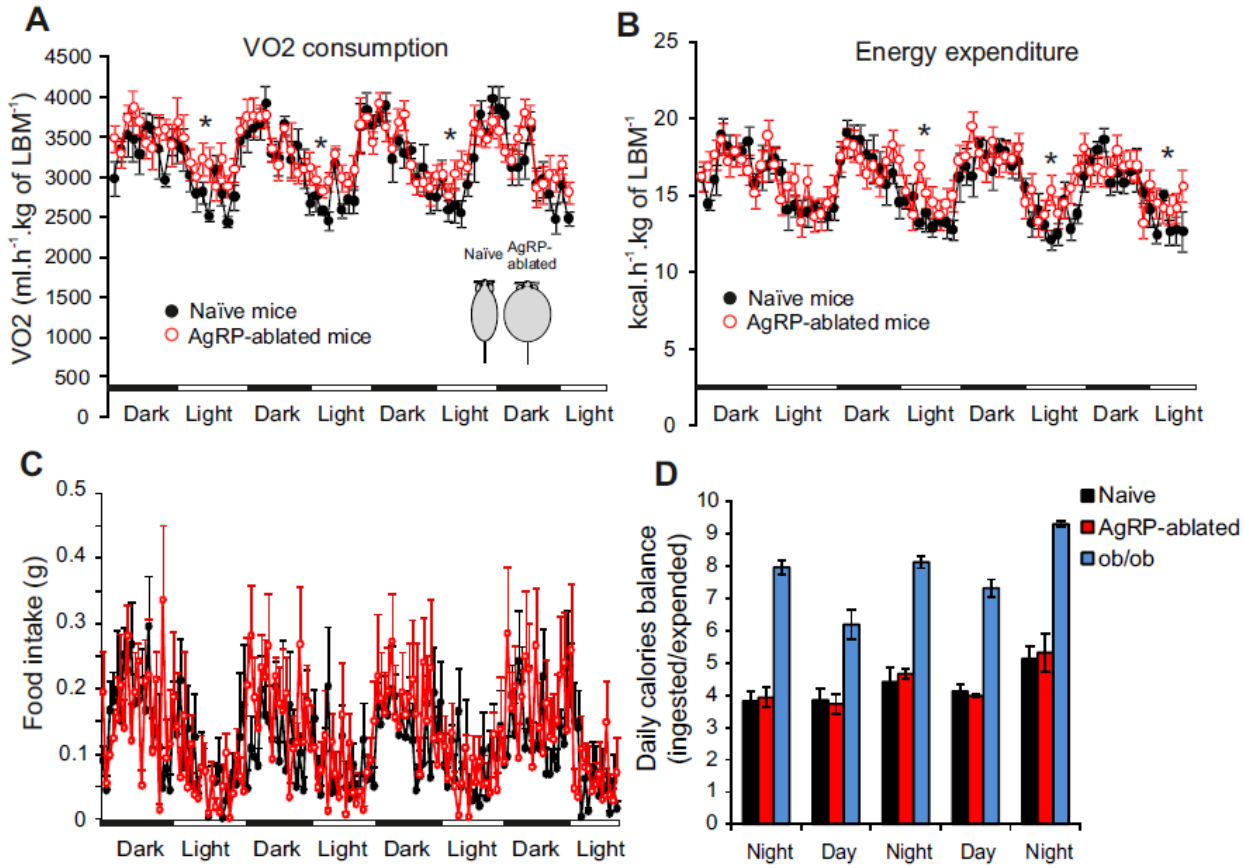

Supplementary Figure 1. Analysis of feeding and energy expenditure.

Oxygen consumption (liter of O_2/hr/kg of lean body mass) (**a**), energy expenditure (kcal/hr/kg of lean body mass) (**b**) and distribution of daily feeding during that period in g of regular chow diet (**c**) in naïve mice (black circles) and AgRP-ablated mice (red circles). Data were acquired on a 4-days basis using phenomaster/labmaster (TSE system, Gmbh, Germany) in 5-6 months old lean naïve (black circles) and obese AgRP-ablated mice (red circles). O_2 consumption and EE were expressed (liter of O_2/hr/kg of lean body mass) and (kcal/hr/kg of lean body mass) using lean body mass (LBM) also called fat free mass measured by NMR (EchoMRI, medical system, Houston, USA) as denominator. (n=6 in each group). A group of 5 months old *ob/ob* mice (blue), obese AgRP-ablated mice (red) and naïve (black) were also analyzed for whole energy expenditure a daily energy balance (total calories intake/whole energy expended) (**d**). (n=3-4) in each group). Displayed values are means ± SEM. **P*<0.05.

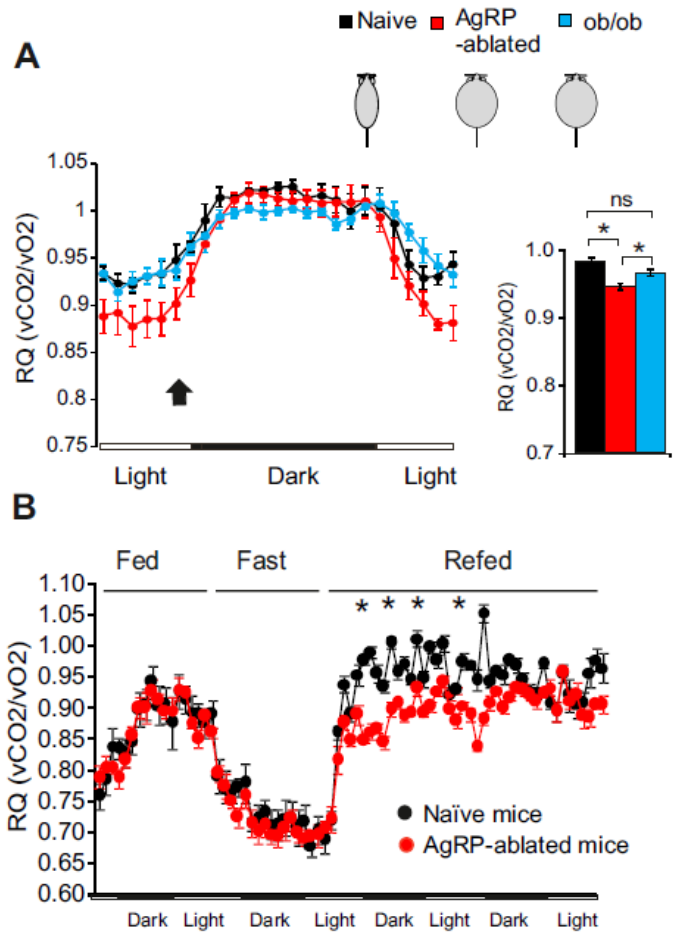

Supplementary Figure 2. Metabolic shift towards lipid oxidation and modified energy expenditure is associated with obesity in AgRP-ablated mice.

Representative distribution of respiratory quotient (VCO_2/VO_2) acquired by indirect calorimetry on the course of several days in naïve (black) and obese AgRP-ablated mice (red) and obese *ob/ob* mice (blue) (**a**). Data are presented as an average of 3 consecutive days (**a-b**) Average RQ value at the entry of the dark cycle, at a time indicated by an arrow, are presented as histogram (* *P* <0.05 using repeated measure ANOVA). Respiratory quotient evolution during basal (**a**), fast and reefed condition (**b**). Data were acquired 5-6 months-old lean naïve animals (black circles); obese AgRP-ablated (red circles) (**a-b**) and *ob/ob* mice (**a**). (n=4-6 in each group). Displayed values are means ± SEM. * *P* <0.05.

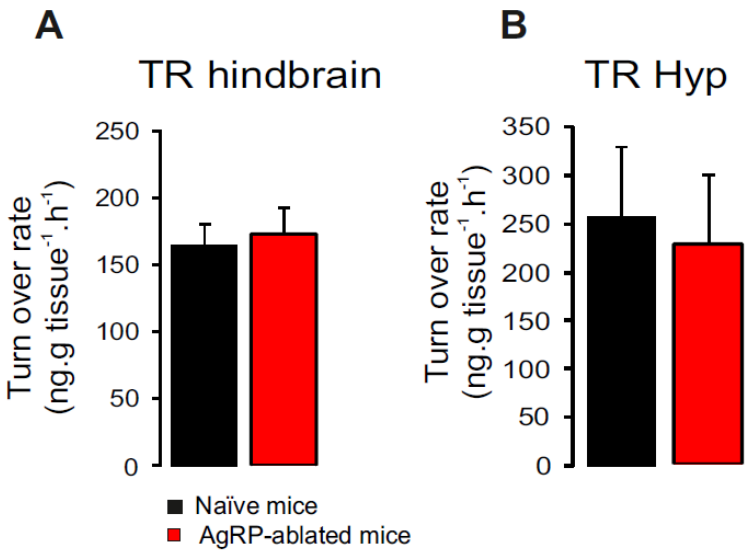

Supplementary Figure 3. Central catecholamine turn-over rate in naïve mice compared to ablated mice.

Catecholamine turn-over rate were (TR) was calculated on Hindbrain (**a**) and hypothalamus (Hyp) (**b**) in lean naïve (black bars) and lean AgRP-ablated mice, (red bars) at a time point that precedes the development of obesity in ablated mice (n=5 in each group). Displayed values are means ± SEM. * $P<0.05$.

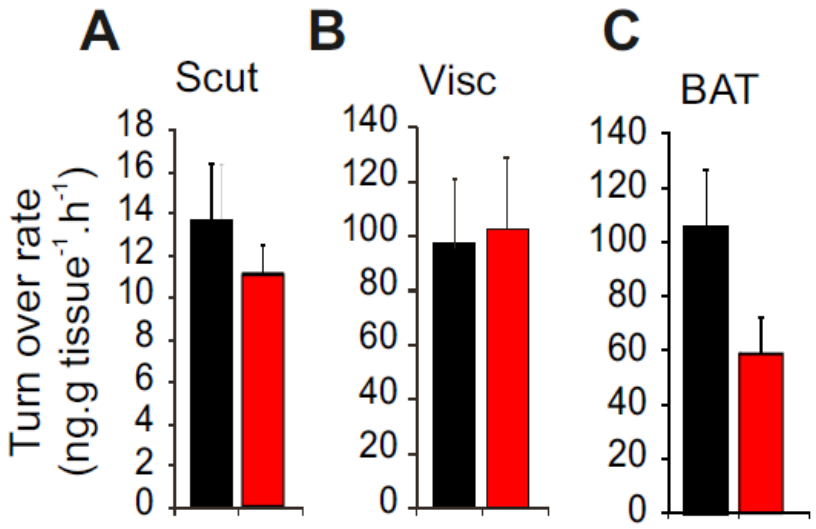

Supplementary Figure 4. Adipose tissue catecholamine turn-over rate in naïve mice compared to ablated mice.

Norepinephrine (NE) turn-over rate (TR) were determined on subcutaneous adipose (**a**) tissue (Scut), Visceral adipose tissue (Visc) (**c**) and brown adipose tissue (BAT) (**c**) in lean naïve (black bars) and lean AgRP-ablated mice, (red bars) at a time point that precedes the development of obesity in ablated mice (n=5 in each group). Displayed values are means ± SEM. * $P<0.05$.

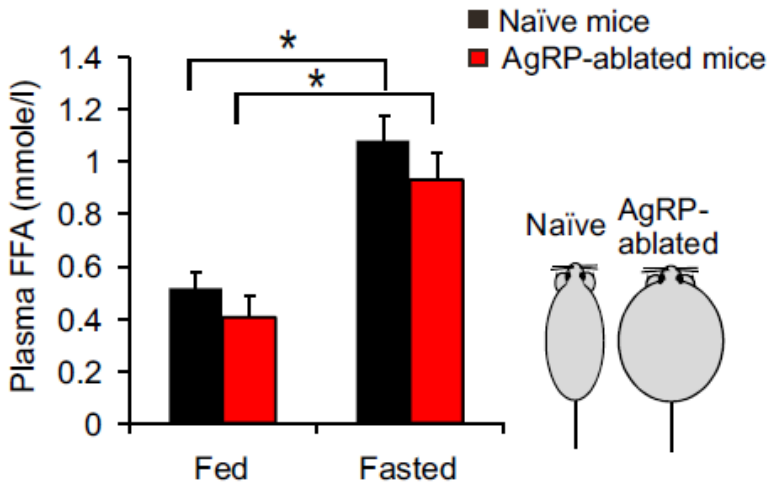

Supplementary Figure 5. Fasting-induced increase of free fatty acids is similar in naïve and AgRP-ablated mice.

Plasma free fatty acids (mM) were measured prior to and after a 24-hr fast**.** These parameters were measured on a group of lean naïve (black bars) and obese AgRP-ablated mice (red bars) (n=6-8 in each group). Displayed values are means ± SEM. * *P* <0.05).

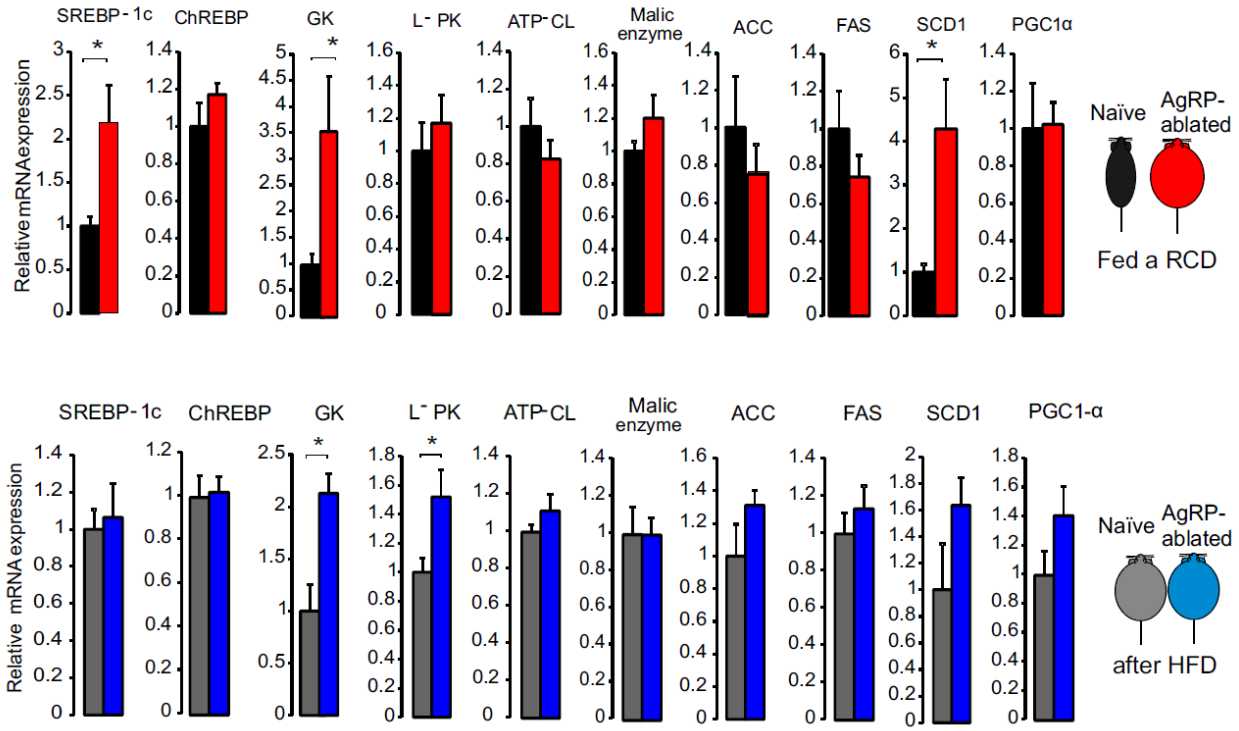

Supplementary Figure 6. Active nutrient conversion in the liver of mice lacking AgRP-neurons under RCD and HFD.

Total liver RNA was extracted and analyzed by qRT-PCR for SREBP-1c (sterol regulatory element binding protein-1c), ChREBP (carbohydrate response element-binding protein), GK (glucokinase), L-PK (L-pyruvate kinase), ATP-CL (ATP citrate lyase), malic enzyme, ACC (acetyl CoA carboxylase), FAS (fatty acid synthase), SCD1 (stearoyl CoA desaturase 1), PGC1α (peroxisome proliferator-activated receptor gamma coactivator 1-α) and PDK4 (pyruvate dehydrogenase isozyme kinase 4) after a 24-hr fast in 6-months old naïve (black and grey bars) and obese AgRP-ablated mice (red and blue bars) under regular chow diet (RCD, upper panel) or after a .6-month high fat diet (HFD, lower panel) (n=7-8 in each group for RCD and .n=4-5 in each group for HFD). Displayed values are means ± SEM. * p <0.05.

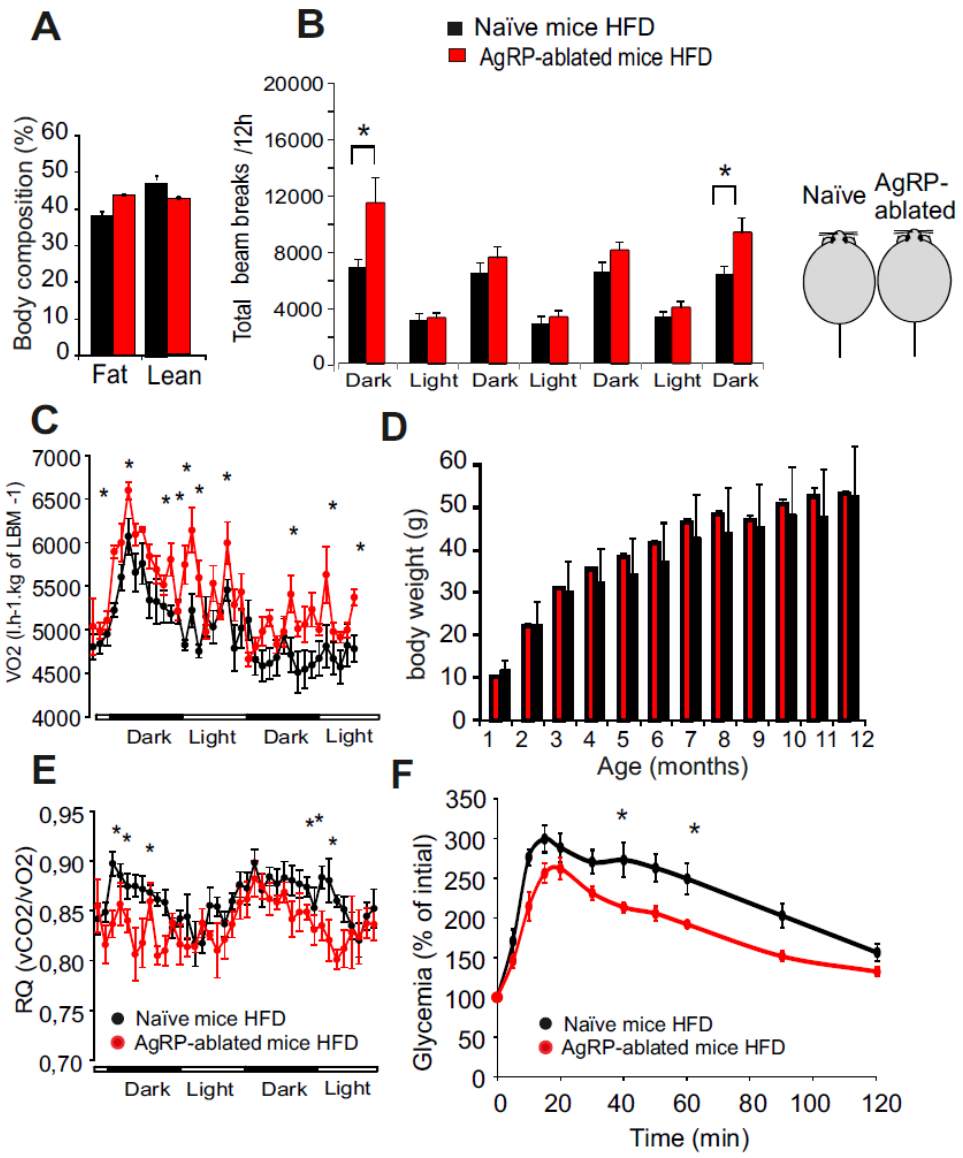

Supplementary Figure 7. Lack of AgRP-neurons is associated with sustained metabolic capabilities during high-fat feeding.

Body composition acquired by NMR (**a**), locomotors activity (**b**), oxygen consumption (**e**) (l of O_2/hr/kg of lean body mass), body weight gain (**d**), representative respiratory quotient analysis (**e**) and blood glucose evolution after an oral charge of glucose (3g/kg) (**f**) in 10 months-old naïve mice (black bars & circles) and AgRP-ablated mice (red bars & circles) after exposure to a high fat diet since the weaning period.. (n=7-4 in each group). Displayed values are means ± SEM. * *P* <0.05.

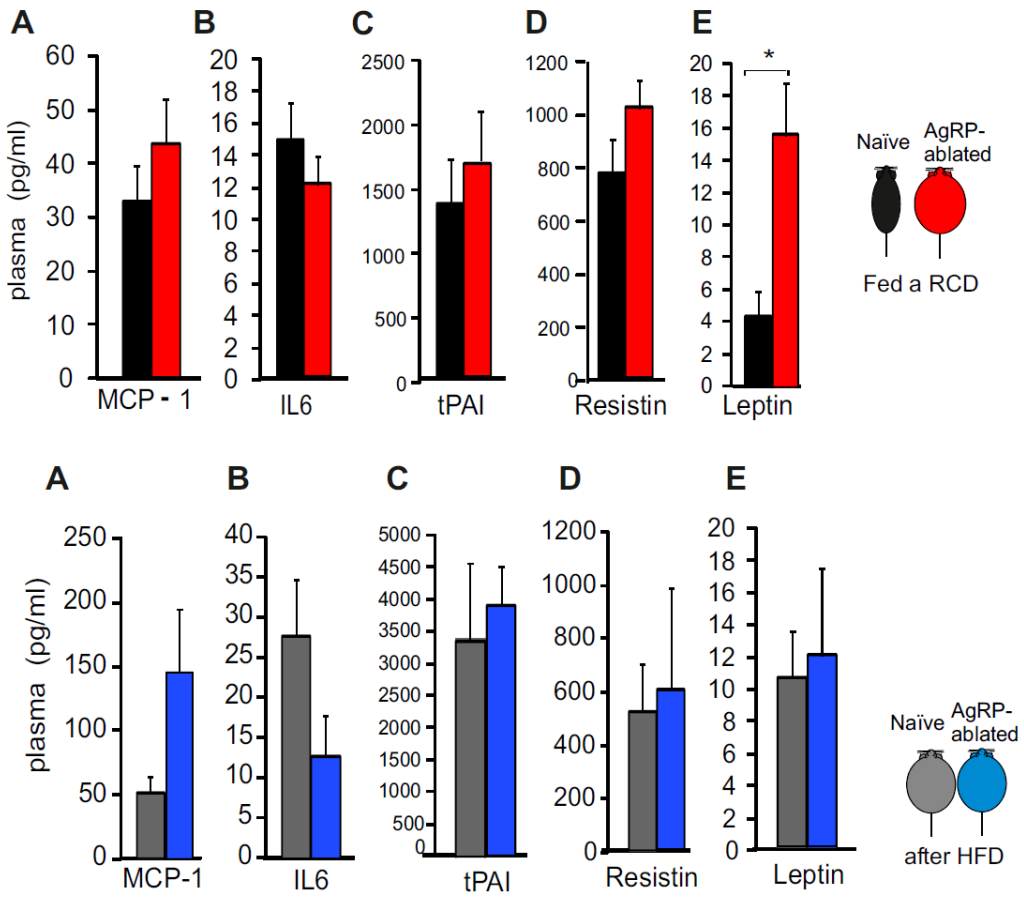

Supplementary Figure 8. Circulating cytokines and hormone in naïve and mice lacking AgRP-neurons.

Plasma level of classic pro-inflammatory cytokines Monocyte chemotactic protein-1 (**a**), (MCP-1), Interleukin-6 (IL6) (**b**), total Plasminogen activator inhibitor-1 (tPAI) (**c**), Resistin (**d**), leptin (**e**) measured after a 24-hr fast in 6-months old naïve (black and grey bars) and obese AgRP-ablated mice (red and blue bars) under regular chow diet (RCD) upper panel or after a .6-month high fat diet (HFD) lower panel (n=7-8 in each group for RCD and .n=4-5 in each group for HFD). Displayed values are means ± SEM. * *P* <0.05.

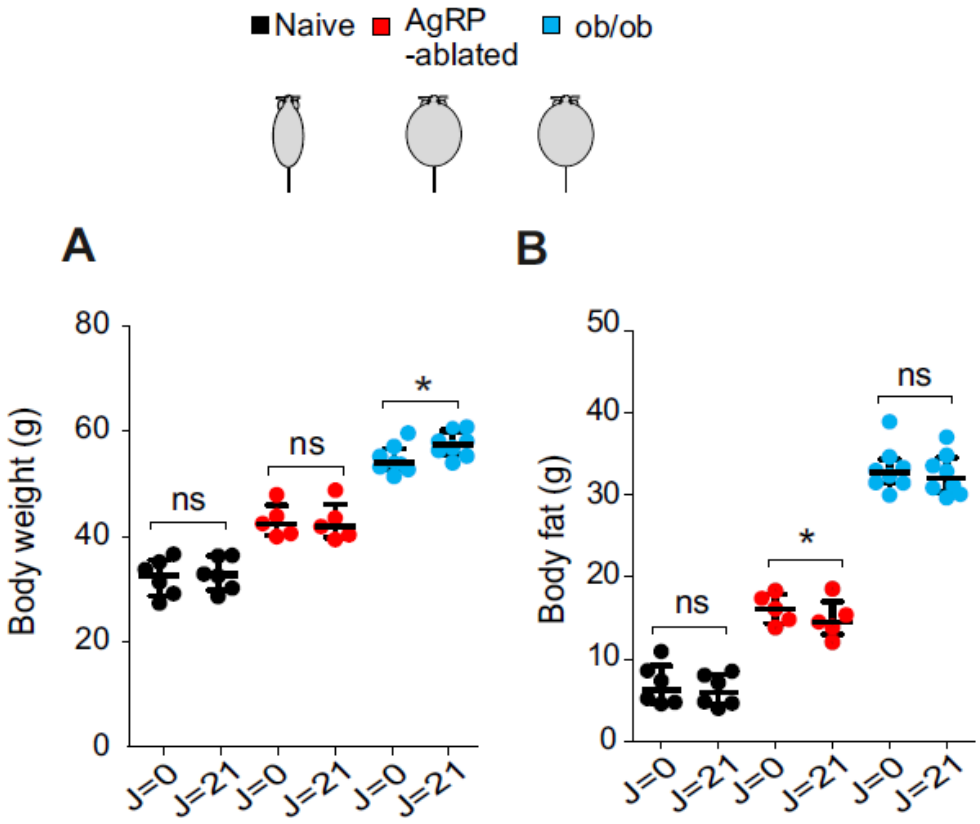

Supplementary figure 9. Mice lacking AgRP neurons develop late onset obesity that has different features compared to *ob/ob* mice.

Body weight (**a**) and body fat content (**b**) was acquired by NMR on naïve (black bars), obese AgRP-ablated mice (red) and obese *ob/ob* (blue) mice prior to (J=0), and 21 days after implantation of subcutaneous osmotic minipumps (mp) delivering the $GABA_A$ receptor partial agonist (0.25µl/hr; 3mg/ml), bretazenil (n=5-8 in each group). Displayed values on the scattered dot plot are median ± interquartile range (* *P* <0.05 using repeated paired student ttest).

Supplementary Table 1. Mitochondrial respiration rates for different complexes of Naïve and AgRP-ablated mice WG and Soleus permeabilized muscle fibers.

	Naïve WG (12)	*AgRP-ablated* WG (12)	*P*
Complex I	7.71 ± 0.65	6.54 ± 0.43	0.14
Complex I+II	12.87 ± 0.78	11.48 ± 0.41	0.13
Complex II	4.65 ± 0.3	4.28 ± 0.18	0.30
Complex IV	16.28 ± 0,99	14.2 ± 0.5	0.079
Ratio CxII/CxI	0.65 ± 0.08	0.68 ± 0.05	0.74
Ratio CxIV/CxI	2.18 ± 0.10	2.25 ± 0.14	0.66
	Naïve Soleus (10)	*AgRP-ablated* Soleus (10)	*P*
Complex I	17.81 ± 1.16	13.21 ± 1.16	**0.037***
Complex I+II	34.,8 ± 1.9	29.32 ± 2.26	0.081
Complex II	15,72 ± 0.54	14,32 ± 1.24	0.319
Complex IV	41,9 ± 2.5	36,01 ± 2.17	0.096
Ratio CxII/CxI	0.97 ± 0.09	1.11 ± 0.06	0.25
Ratio CxIV/CxI	2.51 ± 0.18	2.82 ± 0.15	0.20

Soleus and white gastrocnemius (WG) muscles from 10 month old male mice were analysed (N=6 per group). Complex activity unit is $\mu molO_2.min^{-1}.g^{-1}$ dry weight. Values are given as means together with mean standard error. Number in parentheses is the number of experiments. Each determination is the mean of 1-3 determinations per animal; for statistical analysis unpaired t-test was used and *P* below 0.05 considered as significant, comparison Naïve with AgRP-ablated mice * $P < 0.05$.

Supplementary Table 2. Mitochondrial respiration kinetics in Naïve and AgRP-ablated mice *WG* and Soleus permeabilized muscle fibers in glutamate/malate.

	Naïve WG (12)	*AgRP-ablated* WG (12)	*P*
V_0	1.1 ± 0.07	1.39 ± 0.13	0.067
V_{max}	7.71 ± 0.65	6.54 ± 0.43	0.149
ACR	7.13 ± 0.54	5.05 ± 0.48	**0.008***
	Naïve Soleus (10)	*AgRP-ablated* Soleus (10)	*P*
V_0	3.28 ± 0.24	2.91 ± 0.36	0.40
V_{max}	17.81 ± 1.68	13.21 ± 1.16	**0.037***
$K_{m(aDP)}$	197 ± 22	185 ± 23	0.71
$K_{m(aDP+Cr)}$	40 ± 4.2	45.8 ± 9.12	0.56
ACR	7.1 ± 0.8	4.86 ± 0.4	0,31
$K_{m(aDP)}$. / $K_{m(aDP+Cr)}$	5.06 ± 0.45	5.49 ± 1.11	0.73

Soleus and white gastrocnemius (WG) from 10 month old male mice were analysed (N=6 per group). V_0 and V_{max} unit is $\mu molO_2.min^{-1}.g\ dw^{-1}$. $K_{m(aDP)}$ and $K_{m(aDP+Cr)}$ in µmol. Cr, creatine. ACR, the acceptor control ratio is calculated as V_{max}/V_0. Values are given as means together with mean standard error. Number in parentheses is the number of experiments. Each determination is the mean of 1-3 determinations; for statistic analysis unpaired t-test was used and *P* below 0.05 considered as significant, comparison Naïve with AgRP-ablated mice * $P < 0.05$.

Supplementary Table 3. Mitochondrial substrate utilization in Naïve and AgRP-ablated mice *WG* and Soleus permeabilized muscle fibers.

	Naïve WG (12)	*AgRP-ablated* WG (12)	*P*
Palmitoyl CoA	2.59 ± 0.16	2.66 ± 0.15	0.77
+ octanoate	2.46 ± 0.16	2.47 ± 0.12	0.98
+ pyruvate	6.9 ± 0.37	6.99 ± 0.27	0.85
+ glutamate	8.37 ± 0.36	8.84 ± 0.31	0.33
% fatty acids	29.5 ±1.8	27.93 ± 0.97	0.44
% pyruvate	52.8 ± 2.9	51.4 ± 2.1	0.71
	Naïve Soleus (12)	*AgRP-ablated* Soleus (11)	*P*
Palmitoyl-CoA	13.35 ± 0.64	13.45 ± 0.77	0.91
+ octanoate	13.68 ± 0.61	13.45 ± 0.76	0.81
+ pyruvate	20.52 ± 1.2	16.6 ± 1.0	0.24
+ glutamate	21.1 ± 1.1	18.8 ± 1.1	0.15
% fatty acids	65.4 ± 1.7	72.0 ± 2.4	**0.04***
% pyruvate	31.7 ± 1.9	27.1 ± 2.3	0.15

Soleus and white gastrocnemius (WG) from 10 month old male mice were analysed (N=6 per group). Values are $\mu molO_2.min^{-1}.g\ dw^{-1}$. % fatty acids and pyruvate are normalized to respiration values after glutamate. Values are given as means together with mean standard error. Number in parentheses is the number of experiments. Each determination is the mean of 1-3 determinations; for statistical analysis unpaired t-test was used and *P* below 0.05 considered as significant, , comparison Naïve with AgRP-ablated mice * *P* <0.05.

Supplementary Table 4. list of primers used

SREBP-1c	**5’-ggagccatggattgcacatt-3’** **5’-ggcccgggaagtcactgt-3’**
ChREBP	**5’-gtccgatatctccgacacactctt-3’** **5’-cattgccaacataagcgtcttctg-3’**
GK	**5’-cgactctggggaccgaaggcagatc-3’** **5’-ctcgggtgcagcttgtacacggagc-3’**
L-PK	**5’-cttgctctaccgtgagcctc-3’** **5’-accacaatcaccagatcacc-3’**
ATP-CL	**5’-ctccaaactgtaccgccca-3’** **5’-ggagtgtcctggtagcgcag-3’**
Malic enzyme	**5’-gggcatccctgtgggtaaa-3’** **5’-gaaggcgtcatactcagggc-3’**
ACC	**5’-tgggcacagaccgtggtag-3’** **5’-gtcttaaatgcagagtctgggaa-3’**
FAS	**5’-tgctcccagctgcaggc-3’** **5’-gcccggtagctctgggtgta-3’**
SCD1	**5’-acctgcctcttcgggatttt-3’** **5’-gtcggcgtgtgtttctgaga-3’**
PGC1α	**5’-tgacaaatgctcttcgcttta-3’** **5’-accctgccattgttaagacc-3’**
PDK4	**5’-acgtcctttgcttttctgcg-3’** **5’-gggctttctggtcttctggg-3’**

Supplementary Experimental procedure

C-fos immunostaining

After a 48hr fast mice were anesthetized with pentobarbital and perfused through the left cardiac ventricle 50 ml of Potassium Phosphate Buffer saline 0.1 M solution (PB) at 4°C, followed by 200 ml 4% paraformaldehyde solution, pH 7,4 at 4°C. The brains were removed from the crania and let overnight in paraformaldehyde solutions, and then cryoprotected in PB solution plus 20% sucrose overnight for conservation at -80°C. Brains were then sectioned into 30 µm thick coronal sections and collected in a separate series of wells containing antifreeze solution. Sections of interest of each animal were processed using ABC-DAB techniques against FOS as previously described (Cruciani-Guglielmacci et al, 2004).

Briefly, free-floating sections were incubated for 30 minutes in 3% hydrogen peroxide to inhibit endogenous peroxidase activity and for 6h in blocking solution (0,3 % triton X-100 3% Normal Goat Serum in PBS solution) to block non-specific binding. Tissues were then incubated overnight in a primary polyclonal, rabbit anti-FOS serum (Calbiochem, merck, France) in blocking solution (1:20000) at 4°C. Slices were rinsed in PBS and incubated for a further 1 hour in a secondary, biotinylated, goat anti-rabbit secondary antiserum (Vector Laboratories, Clinisciences, France) in blocking solution 1:2000 at room temperature. The sections were then incubated with avidin-biotin-horsedarish peroxidase complex (Vectastin elite ABC kit, vector laboratories, clinisciences, France) in PBS 0.3% Triton X-100 overnight at 4°C. tissue was then reacted with 3.3'- diaminobenzidine tetrahydrochloride (DAB) as a chromogen. Nickel

ammonium sulfate was used to intensify the reaction product. When FOS staining was sufficient, as established by microscopic examination, the reaction was stopped by rinsing in fresh water. The sections were mounted on superfrost slides. In addition, a negative control was processed at the same time. Omission of the primary antibody results in no staining.

Chromatographic conditions

The samples were analyzed by means of reverse-phase liquid chromatography with electrochemical detection (Waters 2465) at a potential of 750 mV, the detector sensitivity was set at 20 nA. The amine concentrations were calculated from the peak area compared with the peak area of the same compound contained in the external standard solution. Norepinephrine (NA); Epinephrine (aD); Dopamine (DA); 3,4 Dihydroxyphenylacetic acid (DOPAC); Homovanillic acid (HVA) ; 5-Hydroxyindole-3-acetic acid (5-HIAA) ; Serotonin (5-HT), sodium acetate , 1-octanesulfonic acid sodium salt were obtained from Sigma. Perchloric acid, methanol, EDTA disodic from VWR.

The values obtained were expressed as ng/g wet tissue.

The values for the tissue levels of NE and dopamine were logarithmically transformed for calculation of linearity of regression standard error of the regression coefficients and significance of differences between regression coefficients.

Liver lipid analysis.

TG and fatty acids assay were performed by the Lipidomic facility (Inserm U563-CPTP, Toulouse, France). Liver tissue samples were homogenized in 2ml of methanol/ 5mM EGTA (2:1 v/v) with FAST-PREP (MP Biochemicals). The equivalent of 0.5mg of tissue was evaporated, the dry pellets were dissolved in 0.5 ml of NaOH (0.1M) overnight and proteins were measured with the Bio-Rad assay. Lipids corresponding to equivalent of 1mg of tissue were extracted according to Bligh and Dyer (Bligh & Dyer, 1959) in chloroform/methanol/water (2.5 :2.5 :2.1, v/v/v), in the presence of the internal standards : 3 µg of stigmasterol, 3 µg of cholesteryl heptadecanoate, 20 µg of glyceryl triheptadecanoate. Chloroform phase were evaporated to dryness, and dissolved in 20µl of ethyl acetate. 1µl of the lipid extract was analyzed by gas-liquid chromatography on a FOCUS Thermo Electron system using an Zebron-1 Phenomenex fused silica capillary columns (5m X 0,32mm i.d, 0.50 µm film thickness) (Barrans et al, 1994). Oven temperature was programmed from 200°C to 350°C at a rate of 5°C per min and the carrier gas was hydrogen (0.5 bar). The injector and the detector were at 315°C and 345°C respectively.

Lipoproteins analysis.

The HPLC system consisted of a HITACHI L7250 auto-sampler, a L7100 pumps system and two detectors: L7400 (HITACHI) and UVD170U (DIONEX). 20µll of plasma were injected and lipoproteins were separated on Superose^{TM}6 10/300GL column (GE

Healthcare) with 0.15M NaCl solution at a flow rate of 0.4ml/min. The column effluent was split equally into two lines by a microsplitter 50:50, one mixing with cholesterol reagent (BIOLABO) and the other with triglycerides reagent (BIOLABO), thus achieving a simultaneous profiles from single injection. The two enzymatic reagents were each pumped at a rate of 0.2ml/min. Both enzymatic reactions proceeded at 37°C in a Teflon reactor coil (15m X0.4mm id).

Mitochondrial respiration

The mitochondrial respiration was studied in vitro in saponin-skinned fibres as previously described (Athea et al, 2007). Briefly, fibres were separated under a binocular microscope in solution S at 4°C (see below) and permeabilized in solution S with 50 µg/ml of saponin for 30 min. After being placed 10 min in solution R (see below) to wash out adenine nucleotides and creatine phosphate, skinned separated fibres were transferred in a 3-ml water-jacketed oxygraphic cell (Strathkelvin Instruments, Glasgow, UK) equipped with a Clark electrode, as previously described (Athea et al, 2007) under continuous stirring. Solutions R and S contained the following: 2.77 mM CaK2EGTA, 7.23 mM K2EGTA (100 nM free Ca2+), 1 mM free Mg2+, 20 mM taurine, 0.5 mM DTT, and 20 mM imidazole (pH 7.1). Solution S also contained 50 mM potassium-methane sulfonate, (160 mM ionic strength), 5.7 mM Na2ATP, 15 mM creatine-phosphate, while solution R contained 10 mM glutamate, 4 mM malate, 3 mM phosphate, 90 mM potassium-methane sulfonate, 10mM sodium-methane sulfonate (160 mM ionic strength) and 2 mg/ml FA free bovine serum. After the experiments, fibres were

harvested and dried, and respiration rates were expressed as micromoles of O_2 per minute per gram dry weight. Solution R– was similar to solution R without substrates and was used to determine maximal O_2 rates for different substrates.

Measurement of the maximal muscular oxidative capacities

After the determination of basal respiration rate 0 with glutamate-malate as mitochondrial substrates, a submaximal concentration of ADP (100 µM) followed by addition of saturating creatine concentration (20 mM) was added to estimate the sensitivity to ADP of the respiration in the presence or absence of creatine. The maximal fibre respiration rate was measured at 22°C in the presence of saturating concentration of ADP (2 mM) (GM). The acceptor control ratio was GM/ 0 and represented the degree of coupling between oxidation and phosphorylation.

Measurement of the respiratory chain complexes.

When GM was recorded, electron flow goes through complexes I, III, and IV. Then 4 min after this GM measurement, the complex II was stimulated with succinate (15 mM) (complexes I, II, III, IV). Complex I was then blocked with amytal (2 mM). In these conditions, mitochondrial respiration was evaluated by complexes II, III, and IV (S). After that, N,N,N',N'-tetramethyl-p-phenylenediamine dihydrochloride (TMPD, 0.5 mM) and ascorbate (2 mM) were added as an artificial electron donor to cytochrome-c. In these conditions, cytochrome-c oxidase (complex IV) was studied as an isolated step of

respiratory chain (TMPD). The ratios S/ GM and TMPD/ GM allow exploration of complexes I, II, and IV.

Measurement of mitochondrial substrate utilization

Experiments were started in solution R with 4mM malate, 2mM carnitine and 0.1mM Palmitoyl-Coenzyme A. After the determination of basal respiration rate 0, the maximal fibre respiration rate for this fatty acid (PCoA) was measured in the presence of saturating ADP concentration (2 mM). Then substrates were sequentially added as follows: 0.1 mM octanoate, 1 mM pyruvate, and 10 mM glutamate. Each substrate was added during 3 to 4 min. The acceptor control ratio PCoA/ 0 corresponds to the degree of coupling between oxidation and phosphorylation for this substrate. In order to determine the relative contributions of each substrate to respiration rate, the effect of the substrate added previously was subtracted from the cumulative value and values were normalized to the respiration with glutamate/malate.

Plasma chemistry.

Plasma insulin levels were determined by ultra-sensitive mouse insulin ELISA kit (CRYSTAL CHEM, Downer Grove, IL, USA) according to manufacturer protocols. Plasma hormones were assessed using multiplex analysis on luminex technology (Mendo 71k, Millipore for insulin, leptin and glucagon, MADPK 71K for MCP-1, tPAI, resistin, IL6, TNF-α). Plasma FFA was assessed by using NEFA assay kit (Sigma Aldrich, France)

SUPLEMENTARY REFERENCES

Athea Y, Viollet B, Mateo P, Rousseau D, Novotova M, Garnier A, Vaulont S, Wilding JR, Grynberg A, Veksler V, Hoerter J, Ventura-Clapier R (2007) AMP-activated protein kinase alpha2 deficiency affects cardiac cardiolipin homeostasis and mitochondrial function. *Diabetes* **56:** 786-794

Barrans A, Collet X, Barbaras R, Jaspard B, Manent J, Vieu C, Chap H, Perret B (1994) Hepatic lipase induces the formation of pre-beta 1 high density lipoprotein (HDL) from triacylglycerol-rich HDL2. A study comparing liver perfusion to in vitro incubation with lipases. *J Biol Chem* **269:** 11572-11577

Bligh EG, Dyer WJ (1959) A rapid method of total lipid extraction and purification. *Can J Biochem Physiol* **37:** 911-917

Cruciani-Guglielmacci C, Hervalet A, Douared L, Sanders NM, Levin BE, Ktorza A, Magnan C (2004) Beta oxidation in the brain is required for the effects of non-esterified fatty acids on glucose-induced insulin secretion in rats. *Diabetologia* **47:** 2032-2038